Flutter analysis of rotary laminated composite structures using higher-order kinematics

Composites Part C: Open Access 4 (2021) 100100

Contents lists available at ScienceDirect

Composites Part C: Open Access

journal homepage: www.elsevier.com/locate/jcomc

Flutter analysis of rotary laminated composite structures using higher-order kinematics

Raj B. Bharati [a,b], Prashanta K. Mahato [a,*], M. Filippi [b], E. Carrera [b]

[a] Department of Mechanical Engineering, Indian Institute of Technology (Indian School of Mines), Dhanbad 826004, India
[b] MUL2 Group, Department of Mechanical and Aerospace Engineering, Politecnico di Torino, Corso Duca degli Abruzzi 24, Turin 10129, Italy

ARTICLE INFO

Keywords:
Flutter
Rotary wing
p-k method
Advanced 1-D theory

ABSTRACT

The flutter analysis of rotary laminated structures has been performed using Carrera Unified Formulation (CUF). CUF is a one-dimensional higher-order structural model, in which the displacement at the cross-section is the only unknown parameter. The cross-sectional displacement fields of the model are defined using the Lagrange- and Taylor expansion. The quasi-steady and unsteady theories (Theodorsen and Loewy) have been used to apply the aerodynamic force. Subsequently, the equation of motion is defined in 'fundamental nucleus' form using Hamilton's principle. The engineering solution of the flutter condition has been obtained by using *p-k* method. The computational studies of flutter analysis have been done for various rotor hub, lamination sequence, and structural models. The regular, irregular plies and arbitrary fiber orientation of the orthotropic structures have also been considered. The present study suggests that the proposed CUF model can obtain an aeroelastic solution of rotary structure in a computationally and economically efficient manner.

1. Introduction

It is eminent that the study of flutter analysis is essential for the aeroelastic stability of fixed and rotary wing in aircraft, rotorcraft, and spacecraft applications. Flutter appears as dynamic instability, and it can lead to the catastrophic failure of the structure. Hence it should be compulsorily studied by the researcher and designer during the design process. Both fixed and rotary structures are required careful study, but the rotary design needs more focus because of their complexity and structural nonlinearity. These structures require the appropriate idealization of aerodynamic theories with a proper coupling of the structural model to predict the flutter conditions accurately. For the fixed-wing model, aerodynamic theories can be categories as Theodorsen's theory [1] and Greenberg's theory [2]: an extension of Theodorsen's theory that includes the pulsating flow velocity with a constant angle of attack. The rotary-wing can be analyzed by Loewy's theory [3], which includes the unsteady wake behind the reference wing. The failure of wings happens due to the fluid–structure interaction (FSI), and nowadays, due to mechanical and potential advantages of the laminate composite (such as low weight to strength ratio, high specific and structural efficiency) is being used in making wings. The flutter condition can be obtained by analytical, experimental and numerical approach. In the past various numerical approaches have been developed to improve the flutter solution, namely *k, p*, and *p-k* methods [4].

For flutter analysis of fixed-wing, aerodynamic theories based on the strip theory approach are simple and reliable tools [5–8]. For instance, the swept composite wings have been studied to find a laminated structure's aeroelastic characteristics and the author was interested to see the effect of bending-torsion coupling, divergence, tailoring effects, and investigating several aspects of the wings [9,10]. The experimental demonstration study of composite and aluminum plates is available with variation in the sweep in the low-speed wind tunnel for aeroelastic tailoring, divergence, and to compare analytical data with experimental data [11]. The past studies show that the directional property and non-classical effects can influence the aeroelastic instability of structure made of composite materials, and these parameters play a very complex and significant role in flutter and divergence analysis [12,13]. Moreover, many kinds of work have been done in the past few years, where various parameters of wings are considered to analyze the flutter and divergence by wind tunnel tests and computational studies. The evidence found from past tests indicated that structural and aeroelastic non-linearity could influence the flutter condition [14]. Other parameters, such as fiber angle, sweep angle, and density, are also responsible for controlling the flutter conditions [15].

* Corresponding author.
E-mail addresses: raj.bharati@polito.it (R.B. Bharati), pkmahato@iitism.ac.in (P.K. Mahato), matteo.filippi@polito.it (M. Filippi), erasmo.carrera@polito.it (E. Carrera).

https://doi.org/10.1016/j.jcomc.2020.100100
Received 9 December 2020; Accepted 28 December 2020

Flutter analysis of the rotary-wing is more complicated due to the wing's geometrical nonlinearity, and this nonlinearity must need to be including in terms associated with the structure and aerodynamic. Theodorsen [1] developed the theory for 2-D fixed-wing, based on the assumptions of simple harmonic motion of airfoil in incompressible flow by assuming a planner wake behind the wing; however, it has been frequently used for rotary-wing. Later Loewy [3] developed the theory for oscillating rotary-wing, in which approximation of returning wake behind the wing has been taken into account. Loewy's aerodynamics model can be coupled with strip theory to predict the flutter conditions. In the past several studies have been using the v-g method to demonstrate the dynamic instability of isotropic rotary-wings, where the flag-torsional coupling was also included and found that Loewy's theory can capture the wake associated with the wings [16,17]. The structural model of rotary wings can be modeled as a laminated composite, and many works have been done to predict the flutter conditions for these kinds of structural models. The aeroelastic instability analysis for a thin-walled composite rotary wing has also been performed in [18] considering structural coupling due to different ply angles. The nonclassical effects (i.e., transverse and warping) also have been considered in [19] to studied the structural coupling influence on the dynamic instability. The material uncertainty has also been considered in [20] to predict the flutter condition of composite structures. However, small rotor blades and wind turbine blades are inherently different from wings, but some studies of aeroelastic instability are available with different unsteady theories and solving approaches [21–23]. It is observed that limited works have been done on the rotary laminated composite wing with the coupling of different aerodynamic theories and advanced structural models. The aeroelastic analysis of rotary laminated composite wing using *p-k* method is also limited.

This work intends to propose a finite element model (FEM) in Carrera Unified Formulation (CUF) using Lagrange-like expansion and predict flutter conditions of wings (i.e., fixed and rotary) by the *p-k* method. In flutter analysis, the central phenomenon is the interaction between fluid and structures; hence the structural model required the appropriate description of kinematic fields. The structures can be modeled as a plate/beam, and CUF can provide the proper and accurate kinematics fields of plate/beam structures [24]; the initial development of CUF was for plates and shells [25,26]. At present, it has a variety of analyses and applications such as plate, shells, beams, laminated composite, sandwich, thin-walled, and geometrically nonlinear [27–30]. In CUF, both Lagrange- and Taylor-like expansion can be used to interpolate displacement between the beam elements, and the solution obtained by Lagrange and Taylor-like expansion can be improved by increasing the number of nodes and increasing the order of expansion, respectively. Since CUF is a hierarchical formulation, it gives the freedom to choose the order of expansion as the input, and the solution can be improved without changing anything in the formulation. It is also suitable and capable of providing an accurate solution for aeroelastic analysis applications for fixed composite wings using vortex lattice method [31], doublet lattice method [32], piston theory [33], and strip theory [34,35]. Within this work, Taylor- and Lagrange-like expansions have been used to describe the structural model's displacement field in CUF framework. The structural models have been coupled with the aeroelastic model to obtain the motion equation based on Hamilton's principle. The flutter conditions of fixed and rotary wings has been obtained by implementing the *p-k* method within CUF framework.

2. 1-D structural model in CUF framework

A one-dimensional finite element model has been formulated within the Carrera Unified Formulation (CUF) framework, in which the displacement field $u(x, y, z, t)$ states as a combination of cross-section function $F_\tau(x, z)$ and displacement vector $u_\tau(y)$:

$$u(x,y,z,t) = F_\tau(x,z)u_\tau(y) = F_\tau(x,z)N_i(y)q_{\tau i}(t), \quad \tau = 1,2,....,T, \\ q_{\tau i}(t) = \{q_{u_{x\tau i}} \quad q_{u_{y\tau i}} \quad q_{u_{z\tau i}}\} \tag{1}$$

where T, $N_i(y)$, subscript τ and $q_{\tau i}(t)$ stands for number of terms of expansion, shape function, Einstein generalized notation of summation and nodal displacement vector, respectively. In this present work, Eq. 1 contains the Lagrange- and Taylor-like expansion, and structural model has been created using the cross-sectional and beam elements see Fig. 1. The capabilities and details of these expansions can be found in literature [36]; for example displacement field of Lagrange quadratic elements (L9) is:

$$u_x = F_1\, u_{x_1} + F_2\, u_{x_2} + F_3\, u_{x_3} + F_4\, u_{x_4} + ... + F_9\, u_{x_9} \\ u_y = F_1\, u_{y_1} + F_2\, u_{y_2} + F_3\, u_{y_3} + F_4\, u_{y_4} + ... + F_9\, u_{y_9} \\ u_z = F_1\, u_{z_1} + F_2\, u_{z_2} + F_3\, u_{z_3} + F_4\, u_{z_4} + ... + F_9\, u_{z_9} \tag{2}$$

and the compact form and displacement field of Taylor-like expansion for order 'N' is:

$$T = (N+1)(N+2)/2 \\ F_\tau = \left\{F_{(N+1)(N+2)/2} = x^N, F_{(N+1)(N+2)/2} = z^N\right\} \tag{3}$$

for order N=2

$$F_\tau = \{F_1 = 1, F_2 = x, F_3 = z, F_4 = x^2, F_5 = xz, F_6 = z^2\} \tag{4}$$

displacement field:

$$u_x = u_{x_1} + x\, u_{x_2} + z\, u_{x_3} + x^2\, u_{x_4} + xz\, u_{x_5} + z^2\, u_{x_6} \\ u_y = u_{y_1} + x\, u_{y_2} + z\, u_{y_3} + x^2\, u_{y_4} + xz\, u_{y_5} + z^2\, u_{y_6} \\ u_z = u_{z_1} + x\, u_{z_2} + z\, u_{z_3} + x^2\, u_{z_4} + xz\, u_{z_5} + z^2\, u_{z_6} \tag{5}$$

3. Aeroelastic model

3.1. Theodorsen's thoery

This theory is mainly used for the fixed-wing analysis, but also it can be used for unsteady aerodynamic analysis of the rotary-wing. This approach gives the solution of 2-D harmonic oscillations associated with incompressible fluid with assumptions of small disturbance. The lift distribution function was obtained assuming the wing is a flat plate that can rotate about an axis (at distance $x = b_c a$), and the rotation angle is subjected to the angle of attack $\Lambda(t)$, and vertical movement is denoted by $h(t)$. The lift function expressed as [37]:

$$L_a = \pi\rho_a b_c^2\left[\dot{h} + V_\infty\dot{\alpha} - b_c a\ddot{\alpha}\right] + 2\pi\rho_a b_c C(k)V_\infty\left[\dot{h} + V_\infty\alpha + b_c\left(\frac{1}{2} - a\right)\dot{\alpha}\right] \tag{6}$$

where ρ_a, b_c, V_∞, a, $C(k)$ and $k = \frac{\omega b_c}{V_\infty}$ represents the air density, semi-chord, free-stream velocity, pitch axis location, *Theodorsen's function*, and reduced frequency respectively. The above equation contains a non-circulatory (first term) and circulatory terms. *Theodorsen's function* $C(k)$ is equal to 1 and complex function for quasi-steady and unsteady approaches. For unsteady approach $C(k)$ can be expressed in terms of the Hankel function, simplified expression by Jones [38] is:

$$C(k) \equiv 1 - \frac{0.165}{1 - \left(\frac{0.0455}{k}\right)i} - \frac{0.335}{1 - \left(\frac{0.3}{k}\right)i} \tag{7}$$

Since mass properties is absent, first term of Eq. (6) can be neglected and simplified as:

$$L_a \equiv 2\pi\rho_a V_\infty b_c C(k)\left[\dot{h} + V_\infty\alpha\right] \tag{8}$$

The correction of Sectional lift (C_L) associated with the aspect ratio (AR_w) and sweep angle (Λ) has been done by using Diederich's approximation:

$$C_{l\alpha} = \frac{dC_L}{d\alpha} = \frac{\pi AR_w}{\pi AR_w + C_{l\alpha 0}cos(\Lambda)}C_{l\alpha 0}cos(\Lambda) \tag{9}$$

where, aspect ratio is equal to 2 L (wing length)/ c (mean chord), Fig. 2. The lift slope curve is $C_{l\alpha 0} = 2\pi$ and quantity $b_c\pi$ which is slightly inclined and uncamberd has been approximated for pressure distribution

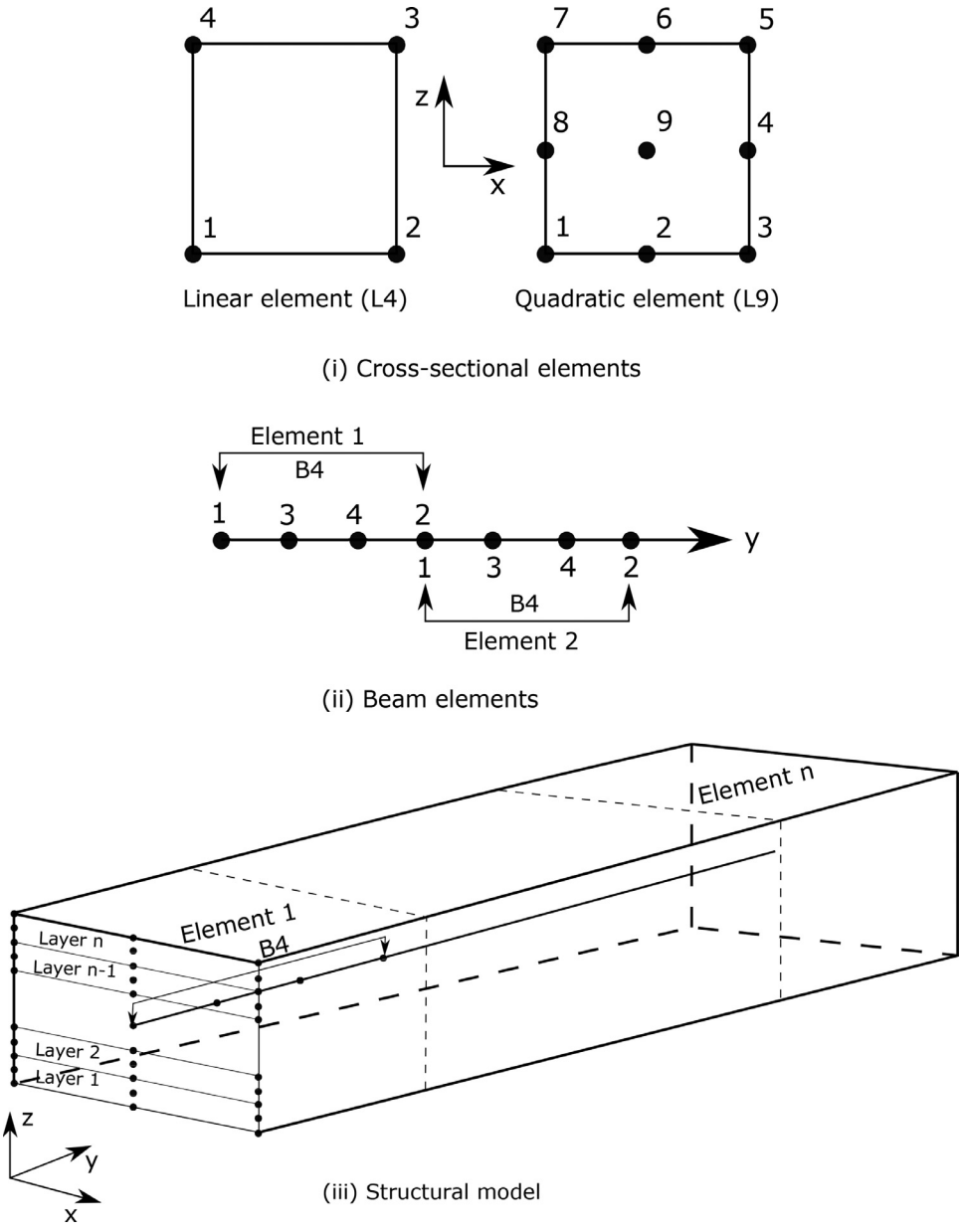

Fig. 1. Structural model in CUF framework.

(on top of thin airfoil) by the $\int_{-b_c}^{b_c}\sqrt{\frac{b_c-x}{b_c+x}}dx$, Eqs. (6) and (8) becomes,

$$L_a = \frac{2\pi\, AR_w\, cos(\Lambda)}{\pi\, AR_w + 2\pi\, cos(\Lambda)} \int_{-b_c}^{b_c} \sqrt{\frac{b_c - x}{b_c + x}} dx\, \rho_a V_\infty C(k) \left[\dot{h} + V_\infty \alpha + b_c\left(\frac{1}{2} - a\right)\dot{\alpha}\right] \tag{10}$$

$$L_a \equiv \frac{2\pi\, AR_w\, cos(\Lambda)}{\pi\, AR_w + 2\pi\, cos(\Lambda)} \int_{-b_c}^{b_c} \sqrt{\frac{b_c - x}{b_c + x}} dx\, \rho_a V_\infty C(k) \left[\dot{h} + V_\infty \alpha\right] \tag{11}$$

3.2. Loewy's thoery

The generalized lift function of a rotary wing expressed as [39]:

$$\frac{dL_a}{dy} = \pi\, \rho_a\, b_c^2\, \Omega^2 \left[\frac{\ddot{h}}{\Omega^2} + \frac{\ddot{\alpha}}{\Omega} - b_c a \frac{\ddot{\alpha}}{\Omega}\right] + 2\pi \rho_a b_c C(k) \Omega^2 \left[\frac{\dot{h}}{\Omega} + y\alpha + b_c\left(\frac{1}{2} - a\right)\frac{\dot{\alpha}}{\Omega}\right] \tag{12}$$

Eq. 12 obtained by modifying the Theodorsen formulation [1] for the rotary-wing and lift-deficiency function $C(k)$ is assumed based on the Loewy formulation [3]. In Theodorsen's 2-D thin airfoil approach, the wake is convected to downstream to infinity, but in rotor-craft work vorticity from the blades and returning wake should be encountered. Loewy acknowledged this fact, and he made a historical and successful attempt to modeled a complex 2-D wing model with the returning wake. This returning wake is modeled as the series of layers with the equal vertical separation (h_l) that depends on a few parameters like the number of blades, semi-chord, and induced velocity (u). Loewy represents the lift deficiency function by replacing the Theodorsen's function, expressed as:

$$C'(k, m, h_l) = \frac{H_1^{(2)}(k) + 2J_1(k)W(k, m, h_l)}{H_1^{(2)}(k) + iH_0^{(2)}(k) + 2[J_1(k) + iJ_0(k)]W(k, m, h_l)} \tag{13}$$

where C'(k), W, $Jn(k)$ and $Hn(k)$ represents Loewy function, wake weighting function, first kind of Bessel and second kind of Hankel

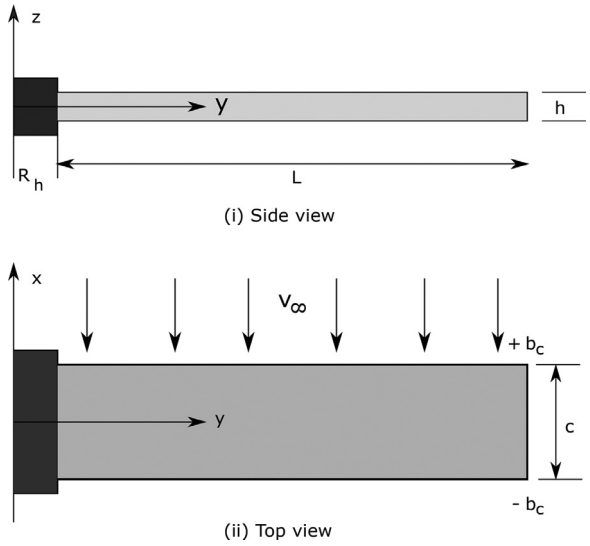

Fig. 2. Reference system for rotary wing

functions, respectively. The value of k and W for a rotor including the 'Q' number of blades is given by

$$k = \frac{2\omega c}{3\Omega R}, \quad W(k,m,h) = \frac{1 + \sum_q^Q (e^{kh_l Q} e^{i2\pi m})^{Q-q} e^{i\Phi q}}{e^{khQ} e^{i2\pi m} - 1} \tag{14}$$

where, R, m, Φ denoted as rotor radius, frequency ratio = ω/Ω (oscillatory-rotational) and phase angle (between refence to q^{th} blades), respectively. Eq. 14 can be written for a single blade with modification of $m \to \hat{m}$ and $h \to \hat{h}$

$$W(k,\hat{m},\hat{h}) = \frac{1}{e^{k\hat{h}Q} e^{i2\pi\hat{m}} - 1}, \quad \hat{m} = \frac{\omega}{\Omega Q}, \quad \hat{h} = \frac{2\pi\lambda_0}{(b/r)Q}, \quad \lambda_0 \simeq \sqrt{C_T/2} \tag{15}$$

where, λ_0, C_T, r and stands for inflow ratio, thrust coefficient and generic radial distance respectively.

4. Equation of motion (EoM)

The Hamilton's principle states that for any time interval the summation of energy (i.e. kinetic and potential) and variation of work exerted by non conservative forces must be equal to zero. It can be expressed as:

$$\int_{t_0}^{t_1} \delta(T - (U + U_{\sigma_0}))dt + \int_{t_0}^{t_1} \delta L_{ext} dt = 0 \tag{16}$$

where, δ, T, $U + U_{\sigma_0}$ and L_{ext} stands for variation of function, total kinetic, potential energy (internal and external forces) and external loads, respectively. The kinetic and potential (internal and external) energy can be expressed as:

$$T = \frac{1}{2}\int_V \rho(\dot{u}^T\dot{u} + 2u^T\Omega^T\dot{u} + u^T\Omega^T\Omega u + 2\dot{u}^T\Omega r + 2u^T\Omega^T\Omega r)dV \tag{17}$$

$$U = \frac{1}{2}\int_V (u^T D^T C D u)dV \tag{18}$$

$$U_{\sigma_0} = \int_V (\sigma_0^T \epsilon_{nl})dV = \int_V ((\Omega^2\rho[R_h R + \frac{1}{2}R^2 - R_h r\frac{1}{2}r^2])^T \epsilon_{nl})dV \tag{19}$$

where,

$$\Omega = \begin{bmatrix} 0 & -\Omega & 0 \\ \Omega & 0 & 0 \\ 0 & 0 & 0 \end{bmatrix} \tag{20}$$

where, matrix D, matrix C, matrix Ω, ρ, r and R_h stands for linear differential operator, material coefficient, rotational speed, density, distance (from neutral axis) and rotor hub radius, respectively.

The external loads can be expressed as:

$$\delta L_{ext} = \int_y\int_x \delta u_z(x,y,z_{top}) L_a(x,y,z_{top})dxdy \tag{21}$$

where, L_a and z_{top} are the lift force and cross-sectional upper z-coordinate. According to Eq. (6) and (12), the Eq. (21) can written for Theodorsen's and Loewy as:

$$L_{ext} = cost\left[\int_y\int_x u^T\sqrt{\frac{b_c - x}{b_c + x}} I_L\dot{u} + u^T\sqrt{\frac{b_c - x}{b_c + x}} I_L u_{,x} + u^T b\left(\frac{1}{2} - a\right)\sqrt{\frac{b_c - x}{b_c + x}} I_L\dot{u}_{,x}\right]dxdy \tag{22}$$

$$L_{ext} = cost\left[\int_y\int_x u^T\Omega y\sqrt{\frac{b_c - x}{b_c + x}} I_L\dot{u} + u^T\Omega^2 y^2\sqrt{\frac{b_c - x}{b_c + x}} I_L u_{,x}\,dxdy + \int_y\int_x u^T\Omega y\sqrt{\frac{b_c - x}{b_c + x}} I_L b\left(\frac{1}{2} - a\right)\dot{u}_{,x}\,dxdy\right] \tag{23}$$

where, $\dot{h} = \dot{u}_z$ $\alpha = \frac{du_z}{dx} = u_{z,x}$ $\dot{\alpha} = \dot{u}_{z,x}$, $cost = \frac{2\pi\, AR\, cos(\Lambda)}{\pi\, AR + 2\pi\, cos(\Lambda)}\, \rho_a U c(k)$ and

$$I_L = \begin{bmatrix} 0 & 0 & 0 \\ 0 & 0 & 0 \\ 0 & 0 & 1 \end{bmatrix}.$$

5. EoM in CUF framework

The kinetic, potential energy and external loads can be derived in the CUF framework (i.e. Fundamental nucleus form). The EoM for the Theodorsen's and Loewy lift function can be expressed as:

$$\int_{t_0}^{t_1} (\delta q_{\tau i}^T M_s^{ij\tau s}\ddot{q}_{sj} + \delta q_{\tau i}^T D_{TT/LT}^{ij\tau s}\dot{q}_{sj} + \delta q_{\tau i}^T K_{TT/LT}^{ij\tau s} q_{sj} + \delta q_{\tau i}^T F_\Omega^{i\tau} r)dt = 0 \tag{24}$$

where, $M_s^{ij\tau s}$ and $F_\Omega^{i\tau}$ are stands for mass matrix and force vector. Whereas subscript 'TT' and 'LT' of $D^{ij\tau s}$ and $K^{ij\tau s}$ are Theodorsen's and Loewy function including the structural and aerodynamic contributions.

The terms associated with subscript 'TT' and 'LT' of Eq. 24 can be expressed as:

$$\begin{aligned} D_{TT}^{ij\tau s} &= D_{aT}^{ij\tau s} + D_{mT}^{ij\tau s} \\ K_{TT}^{ij\tau s} &= K_s^{ij\tau s} + K_{aT}^{ij\tau s} \end{aligned} \tag{25}$$

$$\begin{aligned} D_{LT}^{ij\tau s} &= D_{aL}^{ij\tau s} + D_{mL}^{ij\tau s} + D_\Omega^{ij\tau s} \\ K_{LT}^{ij\tau s} &= K_s^{ij\tau s} + K_{aL}^{ij\tau s} + K_\Omega^{ij\tau s} + K_{\sigma_0}^{ij\tau s} \end{aligned} \tag{26}$$

where, subscript '$a..$' and '$m..$' are aerodynamic contributions. All parameteres of EoM are written below in the form of fundamental nucleus:

$$M_s^{ij\tau s} = I_l^{ij}\int_A (F_\tau \rho I F_s)dA \tag{27}$$

$$F_\Omega^{i\tau} = I_{l_y}^i \lhd F_\tau \rho r \rhd \Omega^T\Omega \tag{28}$$

$$\begin{aligned} K_s^{ij\tau s} = {} & I_l^{ij} \lhd D_{np}^T(F_\tau I)[\tilde{c}_{np}^k D_p(F_s I) + \tilde{c}_{nn}^k D_{np}(F_s I)] \\ & + D_p^T(F_\tau I)[\tilde{c}_{pp}^k D_p(F_s I) + \tilde{c}_{np}^k D_{np}(F_s I)] \rhd \\ & + I_l^{ij,y} \lhd [D_{np}^T(F_\tau I) + D_p^T(F_\tau I)\tilde{c}_{pn}^k] f_s \rhd + I_{Ay} \\ & + I_l^{i,yj} I_{Ay}^T \lhd F_\tau[\tilde{c}_{np}^k D_p(F_s I) + \tilde{c}_{nn}^k D_{np}(F_s I)] \rhd \\ & + I_l^{i,yj,y} I_{Ay}^T \lhd F_\tau \tilde{c}_{npn}^k F_s \rhd \end{aligned} \tag{29}$$

$$
\begin{aligned}
D_{aT}^{ij\tau s} &= cost\ I_l^{ij} \int_{-b_c}^{b_c} \sqrt{\frac{b_c - x}{b_c + x}} F_\tau(x, z_{top})\ I_L\ F_s(x, z_{top})\ dx \\
D_{mT}^{ij\tau s} &= cost\ I_l^{ij} b\Big(\frac{1}{2} - a\Big) \int_{-b_c}^{b_c} \sqrt{\frac{b_c - x}{b_c + x}} F_{\tau,x}(x, z_{top})\ I_L\ F_s(x, z_{top})\ dx \\
K_{aT}^{ij\tau s} &= cost\ I_l^{ij} \int_{-b_c}^{b_c} \sqrt{\frac{b_c - x}{b_c + x}} F_{\tau,x}(x, z_{top})\ I_L\ F_s(x, z_{top})\ dx
\end{aligned} \tag{30}
$$

$$
\begin{aligned}
D_{aL}^{ij\tau s} &= cost\ \Omega\ I_{l_y}^{ij} \int_{-b_c}^{b_c} \sqrt{\frac{b_c - x}{b_c + x}} F_\tau(x, z_{top})\ I_L\ F_s(x, z_{top})\ dx \\
D_{mL}^{ij\tau s} &= cost\ \Omega\ I_{l_y}^{ij} b\Big(\frac{1}{2} - a\Big) \int_{-b_c}^{b_c} \sqrt{\frac{b_c - x}{b_c + x}} F_{\tau,x}(x, z_{top})\ I_L\ F_s(x, z_{top})\ dx \\
D_{\Omega}^{ij\tau s} &= 2\Omega\ I_l^{ij} \int_A (F_\tau \rho I F_s) dA \\
K_{aL}^{ij\tau s} &= cost\ \Omega^2\ I_{l_{y^2}}^{ij} \int_{-b_c}^{b_c} \sqrt{\frac{b_c - x}{b_c + x}} F_{\tau,x}(x, z_{top})\ I_L\ F_s(x, z_{top})\ dx \\
K_{\Omega}^{ij\tau s} &= \Omega^T \Omega\ I_l^{ij} \int_A (F_\tau \rho I F_s) dA \\
K_{\sigma_0}^{ij\tau s} &= \Omega^T \Omega\ I_{l\sigma_0}^{i,yj,y} \int_A (F_\tau \rho I F_s) dA
\end{aligned} \tag{31}
$$

where, $\lhd ....\rhd = \int_A .... dA$

$$
\begin{aligned}
(I_l^{ij}, I_l^{ij,y}, I_l^{i,yj}, I_l^{i,yj,y}, I_{l_y}^{ij}, I_{l_{y^2}}^{ij}, I_{l\sigma_0}^{i,yj,y}) = \int_l (N_i N_j, N_i N_{j,y}, N_{i,y} N_j, N_{i,y} N_{j,y}, \\
y N_i N_j, y^2 N_i N_j, \sigma_0 N_{i,y} N_{j,y})\ dy
\end{aligned} \tag{32}
$$

The EoM can be written in quadratic eigenvalue problem by assuming a periodic solution $q = \bar{q} e^{i\omega t}$:

$$
M\ddot{q} + D_{TT/LT}\ \dot{q} + K_{TT/LT}\ q = 0 \tag{33}
$$

Since matrices of aerodynamic contributions have dependency on the reduced frequency hence an iterative approach is required to calculate the flutter condition. Incorporating the iterative approach Hassig [40] proposed the *p-k* methed to solve the flutter problem. The general and simplified [41] forms of *p-k* are given below

$$
\left[\left(\frac{V_\infty}{c_m}\right)^2 [M_s] p^2 + [K_s] - \frac{1}{2}\rho V_\infty^2 [A(p)]\right]\{q\} = 0 \tag{34}
$$

$$
\left[[M_s]\ p^2 + \left([B_s] - \frac{1}{4}\rho c V_\infty \frac{[Q_a^I]}{k}\right) p + [K_s] - \frac{1}{2}\rho V_\infty^2 [Q_a^R]\right]\{q\} = 0 \tag{35}
$$

where, $[A(p)]$ $[Q_a^I]$ and $[Q_a^R]$ are aerodynamic contribution, imaginary and real part respectively. The value of reduced frequncy (k) is differ for Theodorsen's and Loewy theory.

6. Results and discussion

A Fortran-based FEM code has been developed to obtain the flutter conditions of rotary composite structures. Firstly, isotropic and orthotropic rotary structures were considered for free vibration analysis, and comparison studies performed with available literature. The flutter analysis of the fixed beam structures has also been performed to verify the proposed model. Theodorsen's aerodynamic lift function is used to apply the aerodynamic forces on the structure. The engineering solution has been obtained using the *p-k* method. After analyzing the fixed beam model, the rotary beam model has also been analyzed using quasi-steady, Theodorsen's theory, and Lowey's theory. The Lagrange- and Taylor-like expansion is used to define the kinematics fields of a laminated structural model. Moreover, different rotor hub radius and arbitrary lamination sequences are considered for the rotary beam model to compute the flutter conditions.

Table 1
Geometrical and material properties for rectangular beams.

		Beam 1 Isotropic	Beam 2 6-layer	Beam 3 8-layer	Beam 4 6-layer
Dimensions (mm)	chord (c)	25.4	76.2	76.2	76.2
	thickness (t)	1.6002	0.804*	0.804*	0.804*
	length (l)	444.5	305	305	402
	rotor hub (R_h)	63.5	R_h**	0	0
Material Properties (GPa, Kg/m^3)	E_{11}	68.9	98	144.8	144.8
	$E_{22} = E_{33}$		7.9	9.65	9.65
	ν_{12}	0.3	0.28	0.3	0.3
	$\nu_{13} = \nu_{23}$		0.28	0.3	0.3
	G_{23}		5.6	3.45	3.45
	$G_{12} = G_{13}$		5.6	4.14	4.14
	ρ	2713	1520	1389.23	1389.23

Note: * total thickness of all layers, ** variable parameter

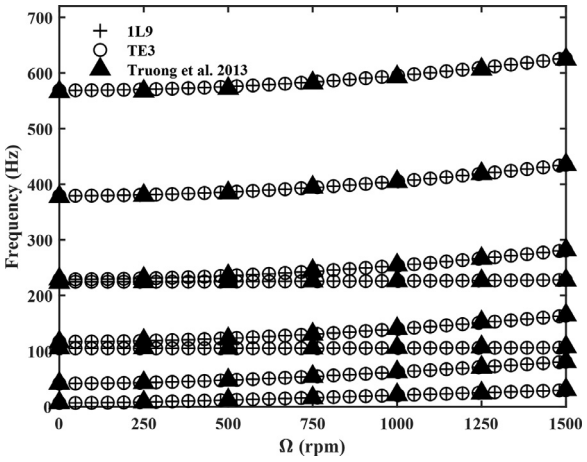

Fig. 3. Comparisons of frequencies of rotating Beam 1.

Table 2
Natural frequencies (Hz) for Beam 2 (6-layers) with lamination $[45/90/0]_s$.

Model	f_{n_1}	f_{n_2}	f_{n_3}	f_{n_4}	f_{n_5}	f_{n_6}	f_{n_7}	f_{n_8}
TE2	4.78	29.59	64.41	83.04	164.33	196.62	277.46	341.60
TE3	4.76	29.51	56.91	82.80	162.94	173.24	270.69	298.45
TE4	4.76	29.42	56.74	82.34	161.75	172.08	268.72	294.29
LE (1L9)	4.77	29.53	56.91	82.87	163.03	173.29	270.79	298.56
LE (2L9)	4.76	29.45	56.77	82.48	162.10	172.14	269.31	294.46
LE (2L9)	4.76	29.43	56.70	82.39	161.88	171.94	268.93	294.02

6.1. Free vibration analysis

The rectangular beam models given in Table 1 are considered for the free vibration analysis. Beam 1 is made of isotropic (aluminum) and Beam 2 made of 6-layers orthotropic materials with lamination sequence $[45/90/0]_s$. Various Lagrange elements (1L9, 2L9 etc.) and different order of Taylor-expansion (TE2, TE4, etc.) used to compute the natural frequency of structural models and cross-sectional elements are shown in Fig. 1. The results obtained for Beam 1 are compared with the 3D beam model [42] and the first 8-modes of frequencies are shown in Fig. 3 with respect to rotational speed. The convergence study has been done for both models; Taylor expansion (TE) was refined by increasing the order of expansion and Lagrange expansion (LE) by increase the number of elements (along the chord). It is observed that third-order of Taylor expansion (TE3) and one nine-noded Lagrange elements (1L9) structural models are best-suited results with the reference. The natural frequencies for the orthotropic beam with the structural model (TE and LE) are reported in Table 2. The first 8-modes of natural frequencies of the TE model are shown in Fig. 4a. It is observed that TE4 is the best-suited model among the other TE models. Moreover, the LE model is

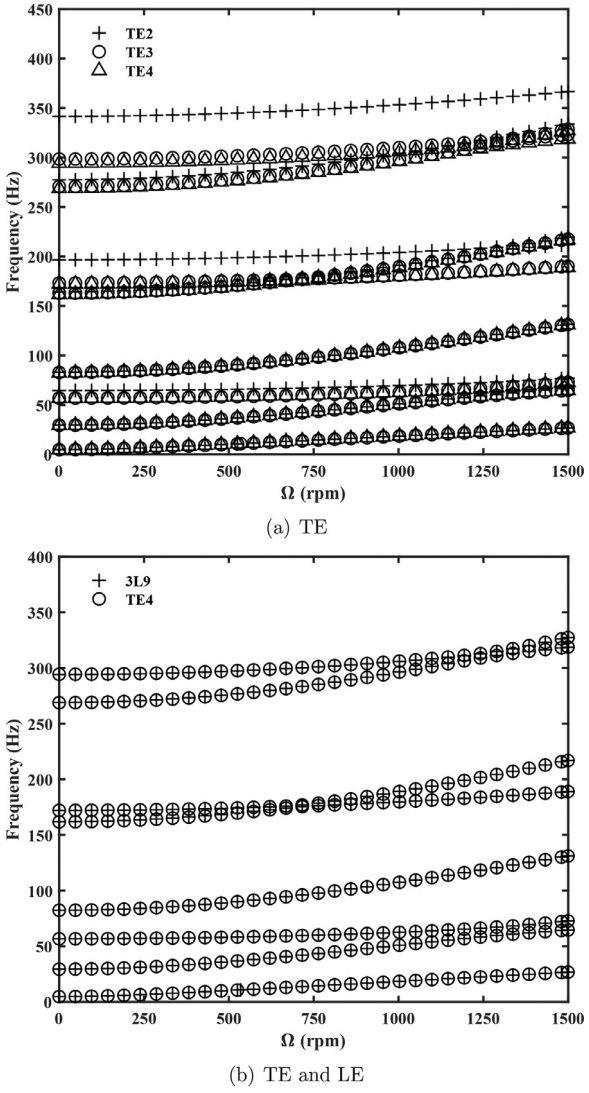

Fig. 4. Frequencies vs rotational speed for Beam 2 with lamination $[45/90/0]_s$.

compared with the TE4 in Fig. 4b and the comparison shows that the 3L9 model enables to compute the natural frequencies as a higher-order model of TE4.

6.2. Flutter analysis

Initially, isotropic (Beam 1) and orthotropic (Beam 2) rectangular fixed beams are considered for the flutter analysis. The geometrical and material properties are given in Table 1. The flutter condition computed using the *p-k* method in the CUF framework. Theodorsen's aerodynamic model was used with structural models (LE and TE) for predicting flutter conditions. Structural models are considered based on the convergence studies performed for free vibration analysis. Various lamination sequences $[30_2/0]_s$, $[45_2/0]_s$ $[30/60/90]_s$, and $[45/90/0]_s$ are considered for Beam 2. The flutter velocity for the both isotropic and orthotropic model are reported in Table 3. The results obtained for lamination sequence $[30_2/0]_s$, and $[45_2/0]_s$ are compared with the analytical and experimental results [43], and good agreement is observed. After verifying the proposed CUF model for the free vibration analysis of the rotating beam and flutter analysis of the fixed beam model, the authors assume that the proposed CUF model can predict flutter conditions accurately for the rotary beam model.

Table 3
Flutter velocities (m/s) for fixed beam model.

		Present		Refrence [43]	
Beam	Lamination	3L9	TE4	Ana.	Exp.
1		124.5	125.7		
2	$[30_2/0]_s$	27.5	26.8	27.8	27
	$[45_2/0]_s$	28.2	27.3	27.8	28
	$[30/60/90]_s$	27.2	26.2		
	$[45/90/00]_s$	30.4	29.3		

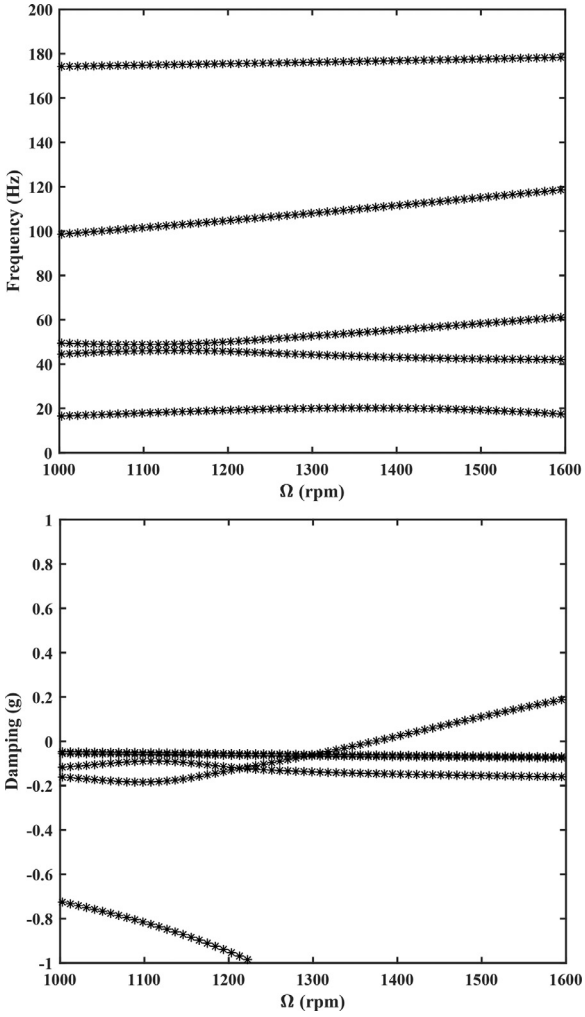

Fig. 5. Flutter diagram for Beam 3 (3L9, $R_h = 45.75\ mm$) with lamination $[45/90/00]_s$.

The flutter analysis of rotary structure is performed for Beam 2, which has 6-layers symmetric laminate $[45/90/0]_s$. The Lagrange expansion (LE) and Taylor expansion (TE) used to define the kinematic fields of the structure. The flutter conditions for both structural models are obtained using quasi-steady (ST), Theodorsen's theory (TT), and Loewy's theory (LT). For LT analysis, the number of blades and the inflow ratio (λ_0) has been assumed equal to 4 and 0.05, respectively. Different radius values considered for rotor hub (R_h) to compute the flutter velocities (Ω_F) and flutter frequencies (f_F), results are reported in Table 4. The flutter diagram (rotational velocity vs. frequency and damping) for the 3L9 model using ST is shown in Fig. 5. It is observed that flutter conditions vary with the radius of the rotor hub and LT is best suited among all aerodynamic models. Also, observed that TE4 and 3L9 are the most accurate among all structural models.

Table 4
Flutter velocity (rpm) and frequencies (Hz) for Beam 3 with lamination $[45/90/0]_s$.

		2L9		3L9		TE3		TE4	
$R_h(mm)$	Theory	Ω_F	f_F	Ω_F	f_F	Ω_F	f_F	Ω_F	f_F
0	ST	1411.4	43.50	1379.9	42.84	1430.5	43.88	1392.3	43.10
	TT	1437.2	42.70	1403.7	42.04	1457.2	43.09	1420.9	42.25
	LT	1152.6	48.50	1144.0	47.99	1162.1	48.83	1146.9	48.18
45.75	ST	1426.7	44.33	1374.1	43.26	1411.4	43.50	1388.5	43.54
	TT	1431.4	43.12	1398.0	42.54	1451.5	43.65	1412.3	42.83
	LT	1303.5	46.92	1279.6	46.27	1320.7	47.29	1290.1	46.56
91.5	ST	1401.8	44.50	1370.3	43.83	1422.8	44.92	1384.6	44.12
	TT	1426.7	43.84	1394.2	43.15	1447.7	44.28	1408.5	43.45
	LT	1294.9	47.07	1271.0	46.44	1311.1	47.46	1281.5	46.72

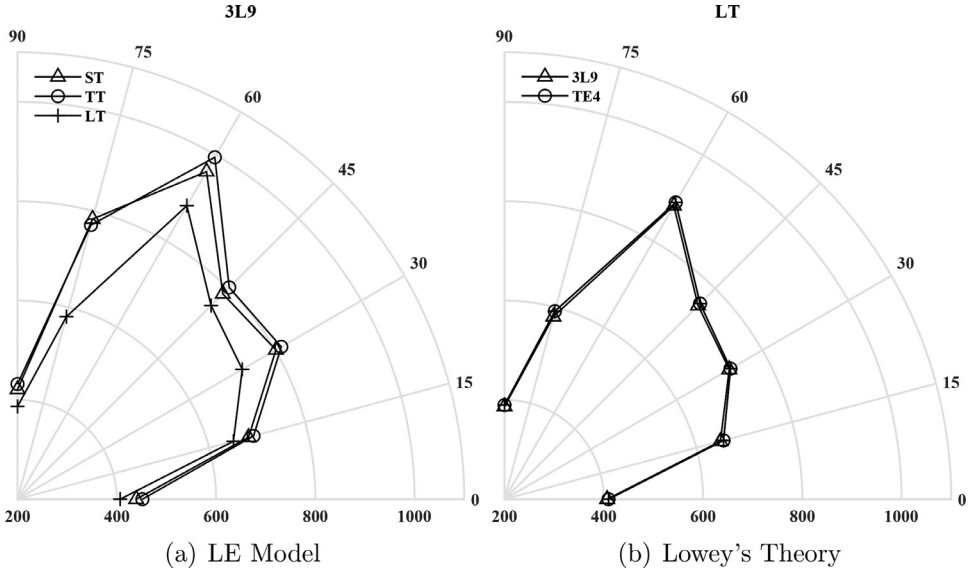

Fig. 6. Polar plot of flutter velocity (rpm) for Beam 5 with arbitrary lamination $[\theta/2\theta/0]_s$.

Table 5
Flutter velocity (rpm) and frequency (Hz) for Beam 4 (8-layers) with lamination $[-22.5/67.5/22.5/-67.5]_s$.

	ST		TT		LT	
Model	Ω_F	f_F	Ω_F	f_F	Ω_F	f_F
2L9	1671.1	54.61	1712.2	53.70	1497.3	58.52
3L9	1632.9	53.94	1673.0	53.00	1469.6	57.90
TE3	1692.1	55.01	1734.2	54.11	1511.7	58.91
TE4	1650.1	54.25	1691.2	53.31	1482.1	58.20

Table 6
Flutter velocity (rpm) for Beam 5 (6-layers) with lamination $[\theta/2\theta/0]_s$.

	θ						
Theory	Model	0°	15°	30°	45°	60°	75°	90°
ST	3L9	439.2	681.8	801.1	784.9	961.6	784.0	421.1
	TE4	448.8	689.4	808.8	790.6	970.2	792.5	424.9
TT	3L9	451.6	692.3	813.6	803.1	995.0	771.5	432.5
	TE4	455.5	700.9	821.2	809.7	1004.6	774.4	437.3
LT	3L9	406.8	650.3	722.8	751.5	882.3	580.6	386.7
	TE4	409.6	656.9	725.7	757.2	889.9	592.0	389.6

In addition, flutter analysis is performed for rotary Beam 3 with irregular plies. The structure assumed have an 8-layers symmetric laminate $[-22.5/67.5/22.5/-67.5]_s$ with irregular plies thickness 0.037, 0.048, 0.064 and 0.253 mm respectively. The flutter conditions obtained for structural models (LE and TE) using quasi-steady and unsteady theories are reported in Table 5. It is observed that TE4 and 3L9 structural models prove to be best suited to predict the flutter conditions, while LT is best suited among all aerodynamic models.

Moreover, the arbitrary value of θ considered to analyze the flutter conditions for Beam 4, which has 6-layers symmetric laminate $[\theta/2\theta/0]_s$. The flutter velocities have been computed using quasi-steady and unsteady theories for refined TE and LE models, which are taken based on the previous analysis. Firstly, the variation range of θ has been considered between 0° to 90° to compute the flutter velocities for both TE and LE models. The flutter velocities are reported in Table 6, and the polar plot for both quasi-steady and unsteady theories for the LE model is shown in Fig. 6a. For a given range of θ, LT results are best suited results compared to others. The comparison between the LE and TE model for LT is shown in Fig. 6b. Where results obtained from both TE and LE models are close to each other. The variation range of θ has been extended from 90° to 180° to compute the flutter velocities for TE4. The flutter velocities obtained using the quasi-steady and unsteady theories, and the polar plot for the range of 0° to 180° is shown in Fig. 7. The obtained results indicate that the LT could predict good flutter conditions in comparison to the others.

7. Conclusion

Flutter analysis of rotary wings has been analyzed using unsteady aerodynamics theories and refined beam theories based on Carrera Unified Formulation (CUF). The *p-k* method was implemented in the CUF framework to obtain the engineering solution of flutter conditions.

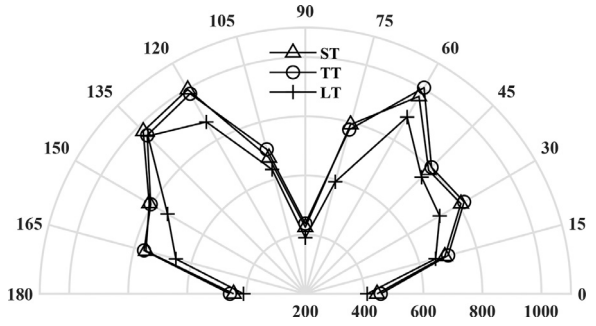

Fig. 7. Polar plot of flutter velocity (rpm) for Beam 5 (TE4) with arbitrary lamination $[\theta/2\theta/0]_s$.

Lagrange elements have also been considered for cross-section discretization in CUF. The numerical simulation and convergence studies have been performed for the proposed model. The model was also verified through the free vibration analysis of rotary-beam and flutter analysis of Fixed-beam. It is found that the present results have a good agreement with the literature. The flutter analysis of rotary-wing was performed considering the various rotor hub, lamination sequence,s and different structural models in CUF using the quasi-steady, Theodorsen, and Loewy theories. The obtained results indicated that the lamination sequence and rotor hub could influence the flutter condition. The present study suggests that the proposed CUF models are enabled to predict the accurate flutter condition as a 3D solution in a computationally and economically efficient manner. In future work, CUF can be used for aerodynamic analysis of swept-wing and forward-flight with complex structural and nonlinearities.

Declaration of Competing Interest

The authors whose names are listed immediately below certify that they have NO affiliations with or involvement in any organization or entity with any financial interest (such as honoraria; educational grants; participation in speakersbureaus; membership, employment, consultancies, stock ownership, or other equity interest; and expert testimony or patent-licensing arrangements), or non-financial interest (such as personal or professional relationships, affiliations, knowledge or beliefs) in the subject matter or materials discussed in this manuscript.

The authors declare that they have no known competing financial interest or personal relationships that could have appeared to influence the work reported in this paper.

Acknowledgment

The work was supported by the SERB, DST, and Govt. of India (Letter no. CRG/2018/004876).

References

[1] T. Theodorsen, General Theory of Aerodynamic Instability and the Mechanics of Flutter, NACA Report 496, 1949.
[2] J.M. Greenberg, Airfoil in Sinusoidal Motion in Pulsating Stream, NACA TN 1326, 1947.
[3] R.G. Loewy, A two-dimensional approximation to the unsteady aerodynamics of rotary wings, J. Aeronaut. Sci. 24 (2) (1957) 81–92. Number: 2
[4] D.H. Hodges, G.A. Pierce, Introduction to Structural Dynamics and Aeroelasticity, 15, Cambridge University Press, 2011.
[5] T. Von Karman, W.R. Sears, Airfoil theory for non-uniform motion, J. Aeronaut. Sci. 5 (10) (1938) 379–390.
[6] W.P. Rodden, B. Stahl, A strip method for prediction of damping in subsonic wind tunnel andflight flutter tests., J. Aircr. 6 (1) (1969) 9–17.
[7] D.S. Jones, The unsteady motion of a thin aerofoil in an incompressible fluid, Commun. Pure Appl. Math. 10 (1) (1957) 1–21.
[8] S.K. Datta, W.G. Gottenberg, Instability of an elastic strip hanging in an airstream, J. Appl. Mech. 42 (1) (1975) 195–198.
[9] T.A. Weisshaar, Divergence of forward swept composite wings divergence, J. Aircr. 17 (6) (1980) 442–448.
[10] T.A. Weisshaar, Aeroelastic tailoring of forward swept composite wings, J. Aircr. 18 (8) (1981) 669–676.
[11] V.C. Sherrer, T.J. Hertz, M.H. Shirk, Wind tunnel demonstration of aeroelastic tailoring applied to forward swept wings, J. Aircr. 18 (11) (1981) 976–983.
[12] L. Librescu, S. Na, Z. Qin, B. Lee, Active aeroelastic control of aircraft composite wings impacted by explosive blasts, J. Sound Vibr. 318 (1-2) (2008) 74–92.
[13] Z. Qin, L. Librescu, Aeroelastic instability of aircraft wings modelled as anisotropic composite thin-walled beams in incompressible flow, J. Fluids Struct. 18 (1) (2003) 43–61.
[14] X. Amandolese, S. Michelin, M. Choquel, Low speed flutter and limit cycle oscillations of a two-degree-of-freedom flat plate in a wind tunnel, J. Fluids Struct. 43 (2013) 244–255.
[15] D.T. Akcabay, Y.L. Young, Material anisotropy and sweep effects on the hydroelastic response of lifting surfaces, Compos. Struct. 242 (2020) 112140.
[16] P. Friedmann, C. Yuan, Effect of modified aerodynamic strip theories on rotor blade aeroelastic stability, AIAA J. 15 (7) (1977) 932–940. Number: 7
[17] P. Friedmann, Arbitrary motion unsteady aerodynamics and its application to rotary-wing aeroelasticity, J. Fluids Struct. 1 (1) (1987) 71–93. Number: 1
[18] R. Ganguli, I. Chopra, Aeroelastic optimization of a helicopter rotor with two-cell composite blades, AIAA J. 34 (4) (1996) 835–841. Number: 4
[19] S.M. Jeon, M.H. Cho, I. Lee, Aeroelastic analysis of composite rotor blades in hover, Comput. Struct. 66 (1 January 1998) (1998) 59–67.
[20] S. Murugan, R. Chowdhury, S. Adhikari, M. Friswell, Helicopter aeroelastic analysis with spatially uncertain rotor blade properties, Aerosp. Sci. Technol. 16 (1) (2012) 29–39.
[21] P.P. Friedmann, Aeroelastic modeling of large wind turbines, J. Am. Helicop. Soc. 21 (4) (1976) 17–27.
[22] J. Sicard, J. Sirohi, Aeroelastic stability of a flexible ribbon rotor blade, J. Fluids Struct. 67 (2016) 106–123.
[23] X. Wei, B.F. Ng, X. Zhao, Aeroelastic load control of large and flexible wind turbines through mechanically driven flaps, J. Frankl. Inst. 356 (14) (2019) 7810–7835.
[24] E. Carrera, G. Giunta, Refined beam theories based on a unified formulation, Int. J. Appl. Mech. 02 (01) (2010) 117–143.
[25] E. Carrera, Theories and finite elements for multilayered, anisotropic, composite plates and shells, Arch. Comput. Methods Eng. 9 (2) (2002) 87–140.
[26] E. Carrera, Theories and Finite Elements for Multilayered Plates and Shells: a unified compact formulation with numerical assessment and benchmarking, Arch. Comput. Methods Eng. 10 (3) (2003) 215–296.
[27] I. Kaleel, M. Petrolo, E. Carrera, A.M. Waas, Computationally efficient concurrent multiscale framework for the nonlinear analysis of composite structures, AIAA J. 57 (9) (2019) 4029–4041.
[28] A. Pagani, M. Petrolo, E. Carrera, Dynamic response of laminated and sandwich composite structures via 1D models based on Chebyshev polynomials, J. Sandw. Struct. Mater. 21 (4) (2019) 1428–1444.
[29] M. Nagaraj, E. Carrera, M. Petrolo, Progressive damage analysis of composite laminates subjected to low-velocity impact using 2D layer-wise structural models, Int. J. Non-Linear Mech. 127 (2020) 103591.
[30] R.B. Bharati, P.K. Mahato, E. Carrera, M. Filippi, A. Pagani, Free vibration and stress analysis of laminated box beam with and without cut-off Recent Adv. Theoret., Appl., Comput. Exp. Mech. 185–196.
[31] A. Varello, E. Carrera, L. Demasi, Vortex lattice method coupled with advanced one-dimensional structural models, J. Aeroelast. Struct. Dyn. (2) (2011) 53–78.
[32] M. Petrolo, Flutter analysis of composite lifting surfaces by the 1D Carrera unified formulation and the doublet lattice method, Compos. Struct. 95 (2013) 539–546.
[33] E. Zappino, E. Carrera, M. Cinefra, Aeroelastic analysis of composite pinched panels using higher-order shell elements, Journal of Spacecraft and Rockets 52 (3) (2015) 999–1003.
[34] M. Filippi, E. Carrera, Aerodynamic and mechanical hierarchical aeroelastic analysis of composite wings, Mech. Adv. Mater. Struct. 23 (9) (2016) 997–1004.
[35] R.B. Bharati, M. Filippi, P.K. Mahato, E. Carrera, Flutter analysis of laminated composite structures using Carrera unified formulation, Compos. Struct. 253 (2020) 112759.
[36] E. Carrera, G. Giunta, M. Petrolo, Beam Structures: Classical and Advanced Theories, John Wiley and Sons.
[37] R.L. Bisplinghoff, H. Ashley, R.L. Halfman, Aeroelasticity, Dover Publication Inc, New York, 1996.
[38] R.T. Jones, Operational Treatment of the Nonuniform-lift Theory in Airplane Dynamics, Technical Report 667, NASA, 1938.
[39] R.L. Bielawa, Rotary Wing Structural Dynamics and Aeroelasticity, American Institute of Aeronautics and Astronautics,, 2006.
[40] H.J. Hassig, An approximate true damping solution of the flutter equation by determinant iteration., J. Aircraft 8 (11) (1971) 885–889.
[41] P.K. Mahato, D.K. Maiti, Aeroelastic analysis of smart composite structures in hygro-thermal environment, Compos. Struct. 92 (4) (2010) 1027–1038.
[42] K.V. Truong, H. Yeo, R.A. Ormiston, Structural dynamics modeling of rectangular rotor blades, Aerosp. Sci. Technol. 30 (1) (2013) 293–305.
[43] S.J. Hollowell, J. Dugundji, Aeroelastic flutter and divergence of stiffness coupled, graphite/epoxy cantilevered plates, J. Aircr. 21 (1) (1984) 69–76.